A robust rabbit model of human atherosclerosis and atherothrombosis

Phinikaridou: Rabbit model of controlled atherothrombosis

Alkystis Phinikaridou [1], Kevin J. Hallock[2], Ye Qiao[1] and James A. Hamilton[*1]

[1] Department of Physiology and Biophysics, Boston University School of Medicine, Boston, MA

[2] Center for Biomedical Imaging, Boston University School of Medicine, Boston, MA

*Author for correspondence

Supplemental Methods and Materials

***In vivo* magnetic resonance images**

In vivo MR images were acquired before and 48 hours after the first pharmacological triggering on a 3 Tesla Philips Intera Scanner using a synergy knee coil in which the sedated rabbits were placed supine. The detailed description of the MR experiments and results will be presented in a future publication. Briefly, cardiac-gated T1-black-blood MR images were acquired using a turbo spin echo sequence to visualize the vessel wall as previously described [1].

Polarized light microscopy to study the melting behavior of lipids in atherosclerotic plaques

The slides were heated and cooled from 20 to 60 °C, in two successive runs, with a rate of 1-2 °C/minute. Digital photographs of the tissue were taken at different temperatures. The onset of melting was defined when the intensity of the birefringence started to decrease and the completion when the birefringence completely disappeared, indicating a liquid-crystal to an isotropic liquid-transition (Heat II). Any crystalline material that remained birefringent at 60 °C and had a needle or plate-like appearance was identified as cholesterol monohydrate crystals (CholM) crystals. Subsequently, the sections were cooled to 20 °C and the temperatures at which the birefringent patterns began to reappear indicated an isotropic to liquid-crystalline (cholesteric or smectic) transition (Cool I). The % birefringence at different temperatures for different types of plaques (n=14) was obtained by processing the digital images using Igor (WaveMetrics, Inc., Lake Oswego, OR) based on the following formula: % birefringence at $temperature_x = Image_{initial}*(Image_{melt}-Image_x)/Image_x*(Image_{melt}-Image_{initial})*100$. $Image_{initial}$=initial image taken before heating, $Image_{melt}$=image taken at completion of heating and $Image_x$=image taken at a temperature between initial and melt.

Supplemental References

1. Phinikaridou A, Hallock KJ, Qiao Y, Hamilton JA. Combining Contrast Enhanced In Vivo and Ex Vivo MRI for Characterizing Vulnerable Plaques in a Rabbit Model of Atherothrombosis. *Proc Intl Soc Mag Reson Med.* 2007; 15:438.

Supplemental Figures

TABLE 1: Medial Changes in Plaques According to the AHA Classification

AHA type	No of sections	Medial breakdown n (%)	Medial fibrosis n (%)	Medial atrophy n (%)	Inflammation of the media n (%)	Neovascularization of the media n (%)
II	27	0	0	0	0	0
III	54	0	0	0	0	0
IV	90	40 (44)	10 (11)	22 (25)	6(7)	40 (44)
Va	81	81 (100)	35 (43)	50 (62)	9 (11)	58 (72)
Vc	36	9 (25)	10 (29)	3 (10)	3 (8)	2 (6)
VI-Ruptured	78	78 (100)	66 (85)	61 (78)	63 (81)	65 (83)
VI-Eroded	22	12 (57)	12 (54)	13 (59)	1 (4)	15 (68)
Total and *P* value	388	<0.001	<0.001	<0.001	<0.001	<0.001
P value Ruptured - Eroded	100	<0.001	<0.001	<0.001	<0.001	<0.001

A. Numbers in parenthesis represent percentages.

Medial breakdown was rare in type Vc ($P<0.001$) plaques but was frequent in types Va and VI-ruptured plaques. Medial fibrosis were rare in type IV plaques and most common in type VI-ruptured plaques ($P<0.001$). Medial atrophy and neovascularization were minimal in type Vc ($P<0.001$) and maximum in VI-ruptured plaques. Medial inflammation was minimal in type IV and frequently present in VI-ruptured plaques. Type VI-ruptured plaques had a higher frequency of medial changes compared to VI-eroded plaques ($P<0.001$).

TABLE 2: Adventitia Changes in Plaques According to the AHA Classification

AHA type	No of sections	Adventitial breakdown n (%)	Inflammation of the adventitia (lymphocytes & plasma cells) n (%)	Neovascularization of the adventitia n (%)
II	27	0	0	0
III	54	0	0	0
IV	90	9 (10)	27 (30)	70 (63)
Va	81	63 (77)	45 (55)	62 (77)
Vc	36	2 (5)	8 (22)	9 (26)
VI-Ruptured	78	70 (90)	72 (92)	69 (88)
VI-Eroded	22	5 (23)	12 (54)	15 (68)
Total and *P* value	388	<0.001	<0.001	<0.001
P value Ruptured-Eroded	100	<0.001	<0.001	<0.001

A. The numbers in parenthesis represent percentages.

Adventitial breakdown, inflammation and neovascularization of the adventitia were absent in types II and III, rare in type Vc and frequent in type VI-ruptured plaques ($P<0.001$). Adventitial changes were more common in type VI-ruptured plaques compared to VI-eroded plaques ($P<0.001$).

Figure I: Physicochemical properties of lipids present in rabbit plaques studied by hot-stage polarized light microscopy

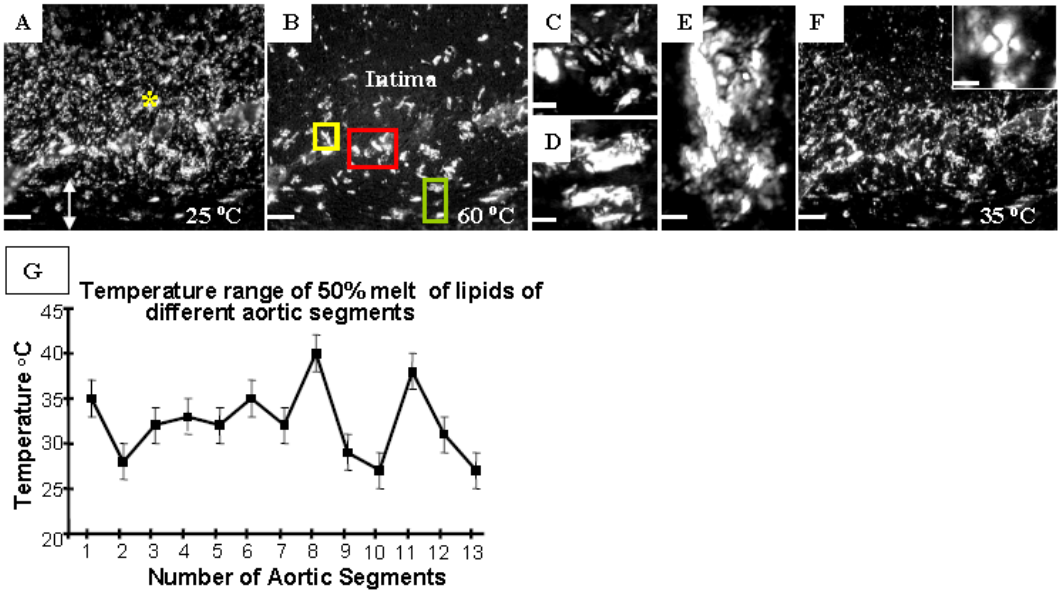

Figures I (A-F) show the melting behavior of a type VI-rupture plaque. **A:** At 25 °C, the lipids are visible within the intima (asterisk) and the media (double arrow). **B:** At 60 °C most of the birefringence disappears indicative of melting of the CE from crystalline to an isotropic liquid. The remaining birefringence corresponds to CholM crystals. **C-D-E:** Higher magnifications of the red, green and yellow boxes shown in II-B identify CholM crystals in the intima (C), CholM crystals in the media (D) and a CholM crystal within a macrophage (E), respectively. **F:** Upon cooling the sample to 35 °C the birefringence reappeared since CE reform liquid crystals, with the characteristic Maltése cross (insert). **G:** The graph shows the melting behavior of lipids in different types of rabbit plaques. 50% of the birefringence disappears between 27-40 °C and thus CE are mainly liquid at body temperature (39 °C). CE: cholesterol ester, CholM: cholesterol monohydrate crystals. Scale bars: 40 µm (A, B, F), 25 µm (C, D, E) and 10µm (6F, insert).

Figure II: Histological example of intraplaque hemorrhage in a rabbit plaque

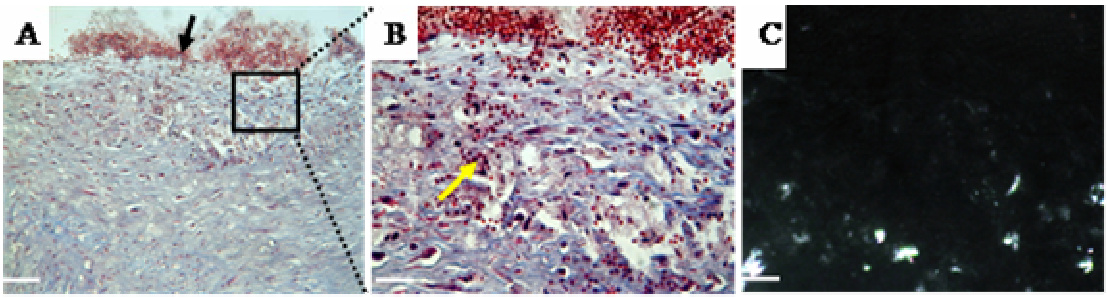

A: Red blood cells within a fibrin mesh are located on the luminal site of a fibromuscular cap. **B:** Higher power view revealed red blood cells scattered within the intima (yellow arrow). **C:** Corresponding polarized light micrograph of an adjacent, unstained section shows that the upper part of the intima is lipid-poor while diffuse lipids are seen within its deeper layers. Masson's Trichrome (A, B), Polarized light microscopy (C). Scale bars: 50 µm; (A), 25 µm (B, C).

Figure III: Correlations between the Plaque Area, Internal elastic lamina area and Lumen area

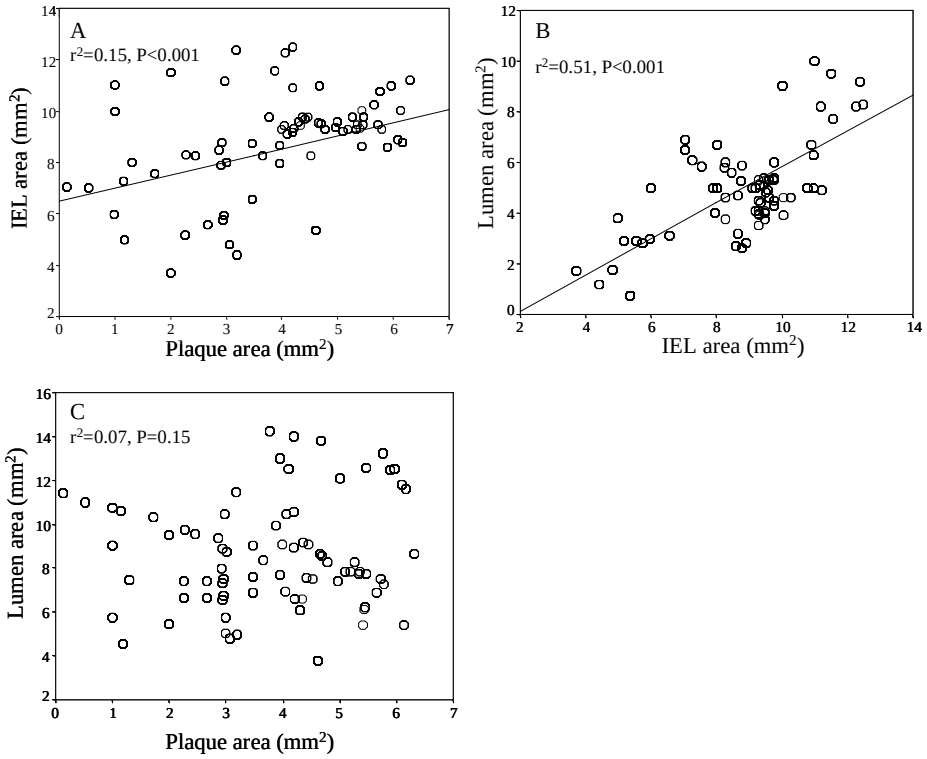

A: There was a linear correlation between the plaque area and IEL area, **B:** There was also a linear correlation between the IEL area and the lumen area, **C:** There was no relation between the plaque area and lumen. IEL: internal elastic lamina.